Available online at www.sciencedirect.com
ScienceDirect
Organic Geochemistry 38 (2007) 1398–1415
Organic Geochemistry
www.elsevier.com/locate/orggeochem

Variations of natural gas carbon isotope-type curves and their interpretation – A case study

Yan-Rong Zou [a,*], Yulan Cai [a], Chongchun Zhang [a,b], Xin Zhang [a,b], Ping'an Peng [a]

[a] *The State Key Laboratory of Organic Geochemistry, Guangzhou Institute of Geochemistry, Chinese Academy of Sciences, Guangzhou 510640, China*

[b] *Graduate School of Chinese Academy of Sciences, Beijing 100039, China*

Received 20 June 2006; received in revised form 1 March 2007; accepted 8 March 2007
Available online 16 March 2007

Abstract

Natural gas is dominated by low-molecular weight gaseous hydrocarbons (C_1–C_5) whose genetic and diagenetic information is mainly obtained from stable carbon isotope compositions. Ordos Basin is one of the largest natural gas provinces in China. By means of examining the carbon isotope compositions of the Ordos basin gases, altered patterns of the isotope-type curves due to secondary cracking, thermochemical sulphate reduction (TSR) and mixing of gases generated from different sources are recognized and discussed. A typical carbon isotope-type curve is nearly linear on the natural gas plot [Chung, H.M., Gormly, J.R., Squires, R.M., 1988. Origin of gaseous hydrocarbons in subsurface environments: theoretical considerations of carbon isotope distribution. Chemical Geology 71, 97–103]. Our results show that the isotope-type curve pattern of TSR and gas secondary cracking in coal is convex due to catalysis, while the isotope-type curve of gas secondary cracking in reservoirs is concave. The natural gas of Yulin, Suligemiao and Wushenqi gas fields is coal-derived gas; both coal-derived gas and mixed gas from oil- and gas-prone sources exist in the Ordovician reservoirs of the Jingbian gas field, depending on the borehole locations. In the Ordovician carbonate reservoirs TSR is recorded but uncommon, whereas secondary cracking in reservoirs is often observed.

1. Introduction

Most of the natural gases accumulated in subsurface reservoirs are generated from thermal degradation of sedimentary organic matter, the origin of which is closely related to diagenetic and thermal alteration of organic matter (Schoell, 1980, 1983). Natural gas, dominated by a few low-molecular weight gaseous hydrocarbons, is compositionally and isotopically simple. As a result of limited molecular complexity, important genetic and post-genetic information is commonly obtained from stable carbon and hydrogen isotope compositions of the hydrocarbons.

Stable carbon isotopic and chemical compositions of natural gases have been used to identify their source organic matter (Schoell, 1980, 1983; Mattavelli et al., 1983; Faber and Stahl, 1984;

* Corresponding author. Tel.: +86 20 85290187; fax: +86 20 85290706.
E-mail address: zouyr@gig.ac.cn (Y.-R. Zou).

0146-6380/$ - see front matter © 2007 Elsevier Ltd. All rights reserved.
doi:10.1016/j.orggeochem.2007.03.002

Whiticar, 1999), the maturity of their source rocks (Stahl and Carey, 1975; Stahl, 1977; Schoell, 1983; Clayton, 1991; James, 1983), their post-generation alteration (Prinzhofer and Huc, 1995; Prinzhofer and Pernaton, 1997; Lorant et al., 1998; Prinzhofer et al., 2000) and reservoir accumulation/loss histories (Tang et al., 2000; Cramer et al., 2001; Zou et al., 2005).

The 'natural gas plot' to identify the origin and mixing of natural gas was proposed originally by Chung et al. (1988). A supplement to this 'natural gas plot' and the potentially altered patterns are provided in this paper.

2. Statistical distribution of stable carbon isotope compositions of gases in Tarim Basin

Tarim Basin, located in NW China, is one of the largest oil- and gas-bearing basins in China. Natural gases in this basin originated both from marine source rocks and coal measures. Statistical results (Jia et al., 2000) for the stable carbon isotope composition of natural gases show that the methane carbon isotope composition has a wide range, from −52.0‰ to −22.0‰ (PDB standard), and a large overlap zone between coal-derived and oil-associated gases (Fig. 1). A trend evident from Fig. 1 is that the carbon isotope values of gaseous hydrocarbons become heavier with increasing carbon number, which is in agreement with Chung et al. (1988). The overlap zone of the isotope values of the C_2–C_4 hydrocarbons from the two sources is relatively narrow, from −26.0‰ to −28.0‰. Dai (1999) reported the stable carbon isotope ranges of gaseous hydrocarbons that discriminate coal-derived from oil-associated gases. For oil-associated gases, the methane carbon isotope compositions range from −55.0‰ to −30.0‰; ethane isotope values are lighter than −29.0‰ and propane isotope ratios lighter than −27.0‰. For the coal-derived gases the methane carbon isotope compositions are between −43.0‰ and −10.0‰; ethane heavier than −27.5‰ and propane heavier than −25.5‰.

The carbon isotope compositions of a large number of individual samples of two kerogen types, oil-prone kerogen collected from the Middle-Upper Proterozoic in North China (Wang and Chen, 2004) and the Jurassic gas-prone kerogen from Kuqa depression in the Tarim Basin, are illustrated in Fig. 2. The carbon isotope compositions for oil-prone kerogens and coaly kerogens range from −34.0‰ to −26.0‰ and −27.0‰ to −22.0‰, respectively. Duan (1995) investigated the carbon isotope composition of 123 coal samples all around China; the results show that the carbon isotope values range from −22.5‰ to −25.5‰ for humic coals and from −28.0‰ to −35.0‰ for sapropelic coals.

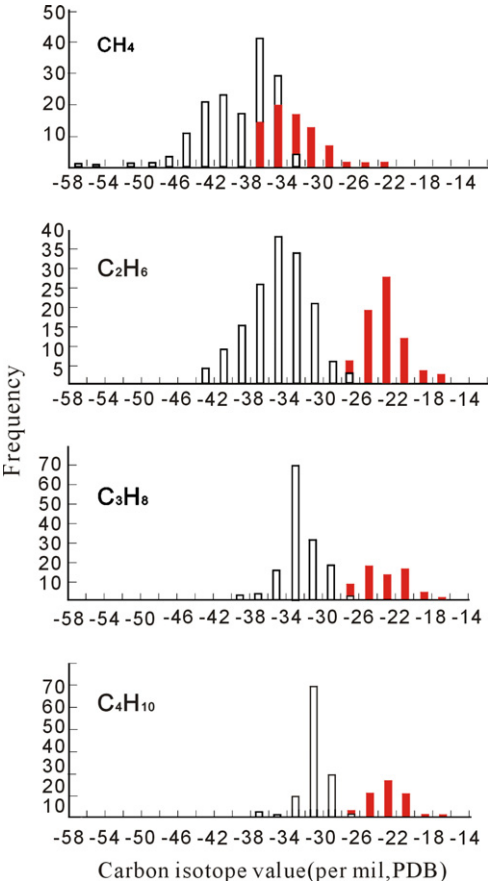

Fig. 1. The statistical distribution of stable carbon isotope composition of natural gases (C_1–C_5) from oil-prone source rocks (open bars) and Jurassic coal measures (solid bars) in the Tarim Basin (after Jia et al., 2000).

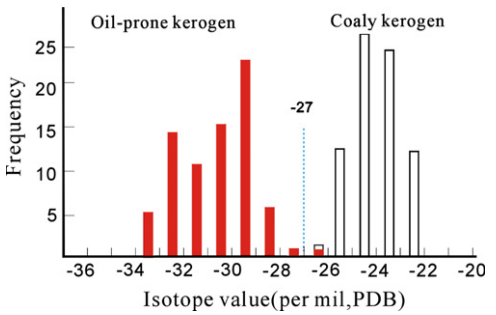

Fig. 2. The carbon isotope compositions of oil-prone kerogen and gas-prone kerogen in northwest China (data after Wang and Chen, 2004).

Table 1
Carbon isotope ranges of different materials and origins

Material	Carbon isotope range		Reference
Gases	Oil-associated	Coal-derived	Dai (1999)
Methane	−55.0‰ to −30.0‰	−43.0‰ to −10.0‰	
Ethane	<−29.0‰	>−27.5‰	
Propane	<−27.0‰	>−25.5‰	
Kerogen	Oil-prone	Gas-prone	Wang and Chen (2004)
	−34.0‰ to − 26.0‰	−27.0‰ to −22.0‰	
Coal	Sapropetic	Humic	Duan (1995)
	−35.0‰ to −28.0‰	−25.5‰ to −22.5‰	

The carbon isotope data mentioned above are summarized in Table 1, which suggest that there is a carbon isotope composition boundary between the oil- and coal-associated gases as well as between the oil- and the gas-prone kerogens that can be used to identify the origin and post-genetic alteration of the gases.

3. Experimental evidence

Pyrolysis techniques are frequently used to simulate hydrocarbon generation and maturation of organic matter. Different techniques have been employed: open system pyrolysis, closed system pyrolysis, and confined system pyrolysis are often reported in the literature. Numerous studies suggest that the gases generated by laboratory simulation of source rock maturation can be compared with field data, and that evidence for organic matter type as well as source rock maturity can be obtained.

In this study, pyrolysis of a type III kerogen isolated from a late Paleozoic coal collected from the Ordos Basin, North China, was performed in a confined system at 20 °C/h. The geochemical characteristics of the coal sample are presented in Table 2. The procedure of the confined pyrolysis was described in detail by Behar et al. (1997). Stable carbon isotope compositions of methane, ethane and propane are presented in Table 3. The carbon isotope data of gases generated during closed system pyrolysis of a Jurassic coal (Liu et al., 2002, 2003) and a calcareous shale (Type I kerogen, Huang et al., 1999) are also listed for comparison. Our results indicate that the gases are enriched in ^{13}C with higher pyrolysis temperatures (maturity increasing) and that the range of carbon isotope values is narrowed with increasing hydrocarbon carbon number. These observations indicate that the lower the carbon numbers of gases, the greater the isotope fractionation between source rock and generated gases, and the higher the maturity, the less the isotope fractionation between kerogen and the gases generated. The trends are consistent with previous studies (James, 1983; Schoell, 1983; Chung et al., 1988).

Berner et al. (1995) performed pyrolysis experiments on algal kerogen and land plant material in an open-system. Hydrous pyrolysis on coal and type II kerogen was carried out by Andresen et al. (1995). Isothermal (24 h) pyrolysis experiments on Type II kerogen in a confined system were carried out by Lorant et al. (1998). Huang et al. (1999) chose a calcareous shale (Type I) and Liu et al. (2003) employed a coal for isothermal (24 h) simulation experiments in a dry, closed-system and Cramer et al. (2001) and Gaschnitz et al. (2001) used coals for the non-isothermal pyrolyses in a dry, open-system. These results of carbon isotope analysis for the generated gases show a trend that gaseous hydrocarbons become enriched in ^{13}C as pyrolysis

Table 2
Geochemical characteristics of coal sample used in confined system pyrolysis experiments

Age code	R_0 (%)	Maceral (vol%)			Element (%)		
		Vitrinite	Exinite	Inertinite	C	H	O
C_{3t}	0.66	55	15	35	71.0	6.8	10.4

Table 3
Carbon isotope compositions of hydrocarbon gases from pyrolysis experiments on coal and marine kerogen

T (°C)	Isotope values (‰PDB)			Remark
	Methane	Ethane	Propane	
380	−33.0	−27.6	−26.2	Confined pyrolysis of Type III kerogen at 20 °C/h this study
401	−35.5	−28.2	−25.7	
421	−36.3	−27.4	−24.9	
442	−35.8	−26.1	−22.5	
484	−33.7	−23.3	−20.7	
505	−32.6	−21.9	−20.4	
325	−47.5	−39.8	−36.0	Closed, isothermal pyrolysis of type I kerogen. Huang et al. (1999)
350	−45.3	−38.1	−36.1	
375	−43.1	−37.7	−35.8	
400	−42.4	−37.2	−34.9	
450	−36.3	−32.7	−29.0	
350	−31.5	−26.7		Closed, isothermal pyrolysis of coal. Liu et al. (2003)
400	−34.2	−25.4	−23.9	
450	−32.4	−23.8	−23.5	
500	−29.7	−22.9	−22.6	
550	−28.6	−21.3		

temperature and the carbon atom number of produced gases increase, very similar to our findings.

4. Altered patterns

4.1. Established patterns

The known patterns of isotope-type curve previously reported (established) alterations of isotope-curve patterns that are mainly attributed to microbial activity. Chung et al. (1988) demonstrated that an unaltered isotope-type curve is nearly linear on the δCn vs. $1/n$ diagram (Fig. 3a). A classic pattern is a variation of this pattern observed for mixed (biogenic–thermogenic) gas, as demonstrated by Chung et al. (1988), Katz et al. (2002), Burruss et al. (2003), Sassen et al. (2003), Pohlman et al. (2005), and Hosgomez et al. (2005). This pattern shows a sharp decrease of the methane isotope value as compared to the unaltered isotope curve (Fig. 3b). Another alteration pattern related to microbial activity is bacterial oxidation, which results in a ^{13}C enrichment of the higher molecular-weight hydrocarbon gases (C_{2+}, especially propane) and a depletion of the methane (Fig. 3c), such as the cases given by

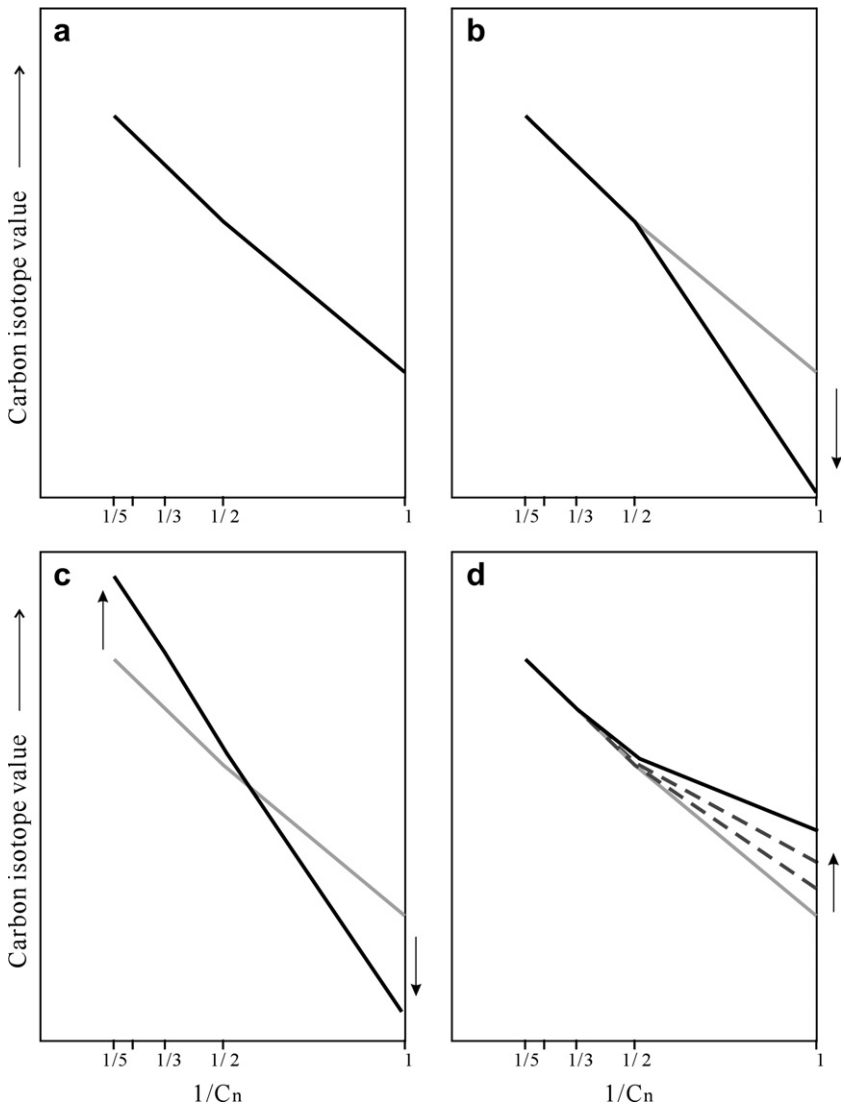

Fig. 3. The known patterns of the carbon isotope-type curves altered. (a) Unaltered; (b) mixed with biogenic gas; (c) bacterial oxidation; (d) methane leakage/diffusion.

Pallasser (2000) and Burruss et al. (2003). Gas leakage/diffusion has also been proposed to alter of the isotope-type curve. Generally, the carbon isotope values of remaining methane becomes less negative, the residual gas would be enriched in ^{13}C with increasing diffusion time in proportion to the progress of the diffusive leakage process (Fig. 3d), as illustrated by Clayton et al. (1997) and Prinzhofer and Pernaton (1997).

4.2. New characteristic patterns

Based on the statistical and experimental data, an improved interpretation of the "natural gas plot" is proposed in this paper. The potential examples for characteristic deviations from the established patterns of the 'natural gas plot' of Chung et al. (1988) and carbon isotope range boundaries of the gases generated from different kerogen types are given in order to identify the gas origins and their post-genetic alteration.

The two potentially systematic variations of the isotope-type curve patterns are related to the thermal stress that gases experienced in their source rock or gas reservoir, i.e. hydrocarbon gas cracking (secondary cracking) and thermochemical sulphate reduction (TSR). When the gases continue to undergo thermal stress after formation, the isotope-type curves patterns may change. We performed several pyrolysis experiments with coaly kerogen in a confined system at heating rates of 2–20 °C/h. Cracking of heavy hydrocarbon gas occurs between 450 and 480 °C, depending upon the heating rate (Table 3). Isothermal pyrolysis experiments on Type II kerogen in a confined system (Lorant et al., 1998) and on Type I kerogen in

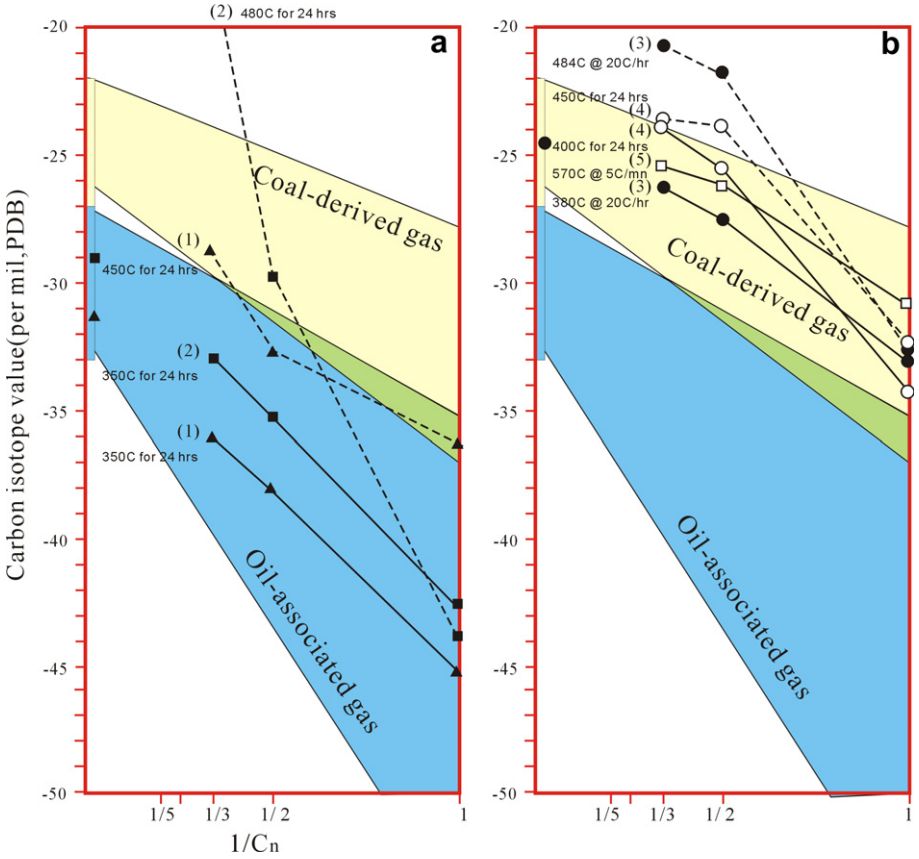

Fig. 4. The pattern of carbon isotope-type curve from oil-prone source rocks (a) and coals (b). The isotope-type curves of mature gas are nearly linear irrespective of their source rocks, whereas the curves are concave for overmature oil-associated gases and convex for overmature coal-derived gases. Solid line: isotope curve of gas generation; dashed line: isotope curve shift due to secondary cracking. (1) Type I kerogen (solid triangle, Huang et al., 1999); (2) Type II kerogen (solid square, data after Lorant et al., 1998); (3) Type III kerogen (solid circle, this study); (4) coal (open circle, Liu et al., 2003) and (5) xylite heated in open-system (open square, data after Berner et al., 1995).

a dry, closed-system (Huang et al., 1999) show that secondary cracking occurred in a similar temperature range. The typical pattern of the carbon isotope curve due to secondary cracking is illustrated in Fig. 4, which demonstrates that when the gaseous hydrocarbons are cracked, the dryness (C_1/C_{1-5}) increases (i.e. the portion of heavy hydrocarbon gases decreases) and the carbon isotope compositions of the residual C_{2+} gases shift towards a positive direction becoming enriched in ^{13}C due to preferential cracking of ^{12}C–^{12}C bonds in C_{2+} alkanes. The carbon isotope composition of methane shows a small negative shift. The carbon isotope values of ethane and propane are heavier than those of their parent rocks, though the methane isotope composition is still within its isotope range. In addition, with secondary cracking a downward "concave" curve is displayed for oil-prone kerogen (Fig. 4a), whereas an upward "convex" curve is shown for gas-prone kerogen (Fig. 4b). This relationship is inferred to be associated with organic macromolecular catalysis. The pattern of the isotope-type curve may be modified by TSR in carbonate reservoirs, which will be discussed in Section 5.

Admixture of high maturity gas may also alter the isotope-type curve. Because high maturity gas is dominated by isotopically heavier methane, mixing results in a shift of methane isotopic composition towards heavier values. The characteristic patterns resulting from mixing of gases from mature type II and type III kerogen and from high maturity type II and type III kerogen are shown in Fig. 5. These data demonstrate that the mixing of gases from mature type II and type III kerogen changes the slope of the isotope-type curve, resulting mainly in a heavier methane isotope (Fig. 5a) which depends on the amount of coal-derived gas. The mixture of gases from high maturity type II and type III kerogens have relatively heavy isotope values for both methane and propane (Fig. 5b). The calculated results (Fig. 5) are similar to the cases provided by Hosgomez et al. (2005).

The mixing calculation of oil-and coal-associated gases suggests that the methane carbon isotope composition of the mixed gas mainly is

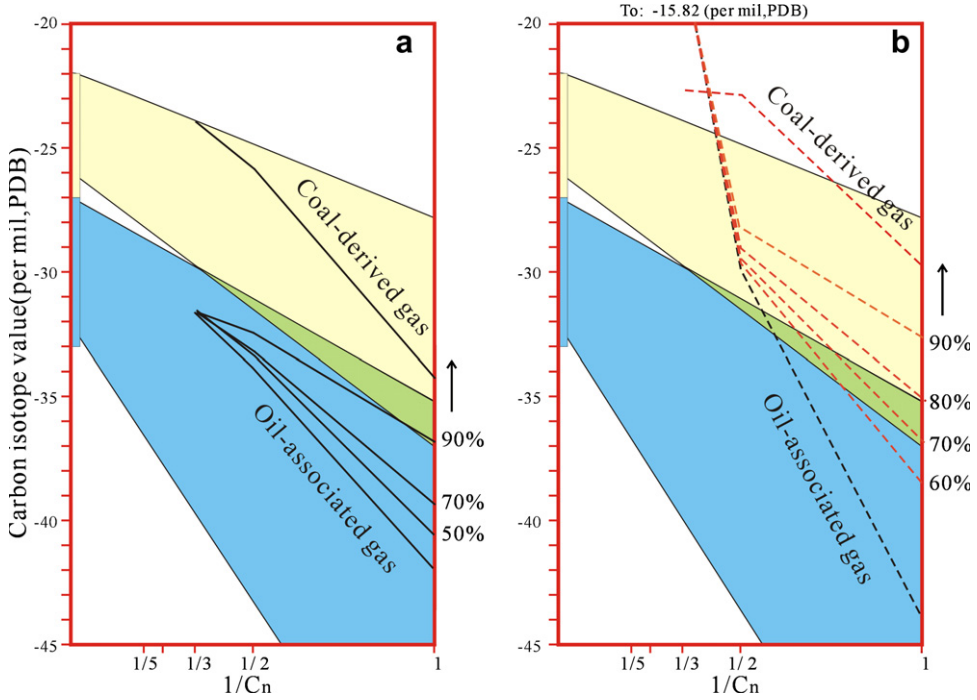

Fig. 5. Isotope-type curves showing the patterns altered by the mixing of gas from mature type II and type III kerogen (solid line) and from overmature type II and type III kerogen (dashed line). Mixing of gases from mature type II and III kerogen changes the slope of the isotope-type curve less (a); a concave curve indicates mixing of the gas mixture from highly mature type II and type III kerogens (b). The gases components and carbon isotope compositions of pyrolysates of mature (400 °C) and high maturity (480 °C) type II kerogen are after Lorant et al. (1998), and those of high maturity (500 °C) coal are after Liu et al. (2002, 2003), respectively.

controlled by the composition of the coal-derived gas, while the carbon isotope compositions of C_{2+} hydrocarbons rely on the oil-associated gas. This is because the coal-derived gas is richer in methane and the oil-associated gas is relatively richer in C_{2+} hydrocarbons. The potentially altered isotope-type curves linked to high temperature are very different from the conventional patterns mentioned above. The characteristic patterns are summarized in Fig. 6.

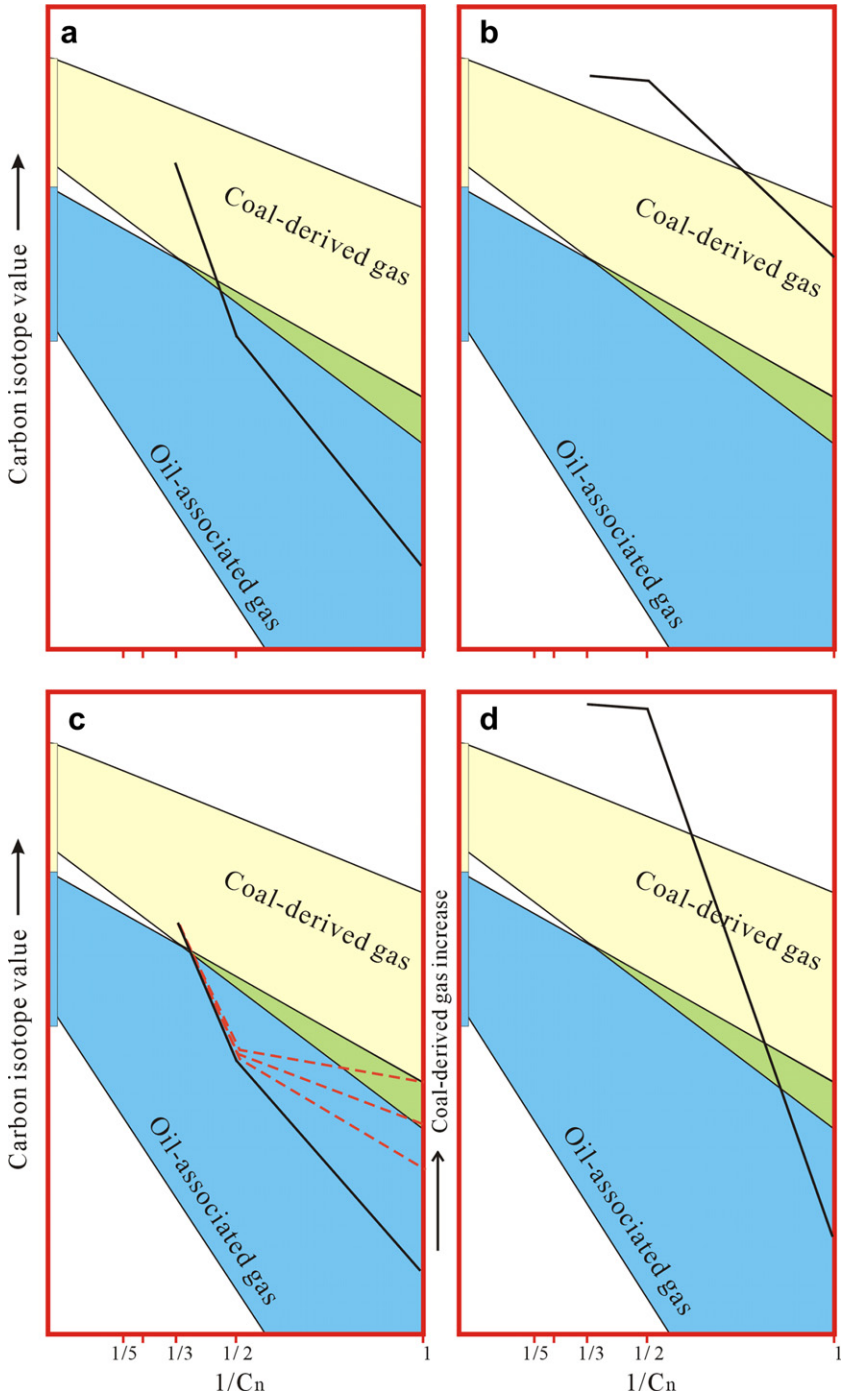

Fig. 6. Schematic patterns of isotope-type curves associated with high thermal stress. (a) Oil-associated gas with high maturity; (b) coal-derived gas with high maturity; (c) mixed oil- and coal-associated gases; (d) isotope-type curve pattern of TSR.

5. Case study and discussion

5.1. Geological setting

The Ordos Basin, with an area of over 250,000 km^2, is the second largest sedimentary basin in China and also one of the China's largest natural gas provinces (Fig. 7). Four giant gas fields, containing more than 100 billion cubic meters of proven gas reserves, have been discovered in the shallow Ordovician and the Carboniferous–Permian (C–P) strata in the northern part of this basin (Dai et al., 2005). A simplified stratigraphic system is shown in Table 4. Yulin, Wushenqi and Suligemiao gas fields have gas reservoirs in the Permian sandstone reservoirs, while the reservoir strata of the Jingbian gas field is mainly the Ordovician weathered carbonate (i.e. the so-called weathered crust) close to the Carboniferous/Ordovician unconformity. Tables 5 and 6 present the carbon isotope composition of natural

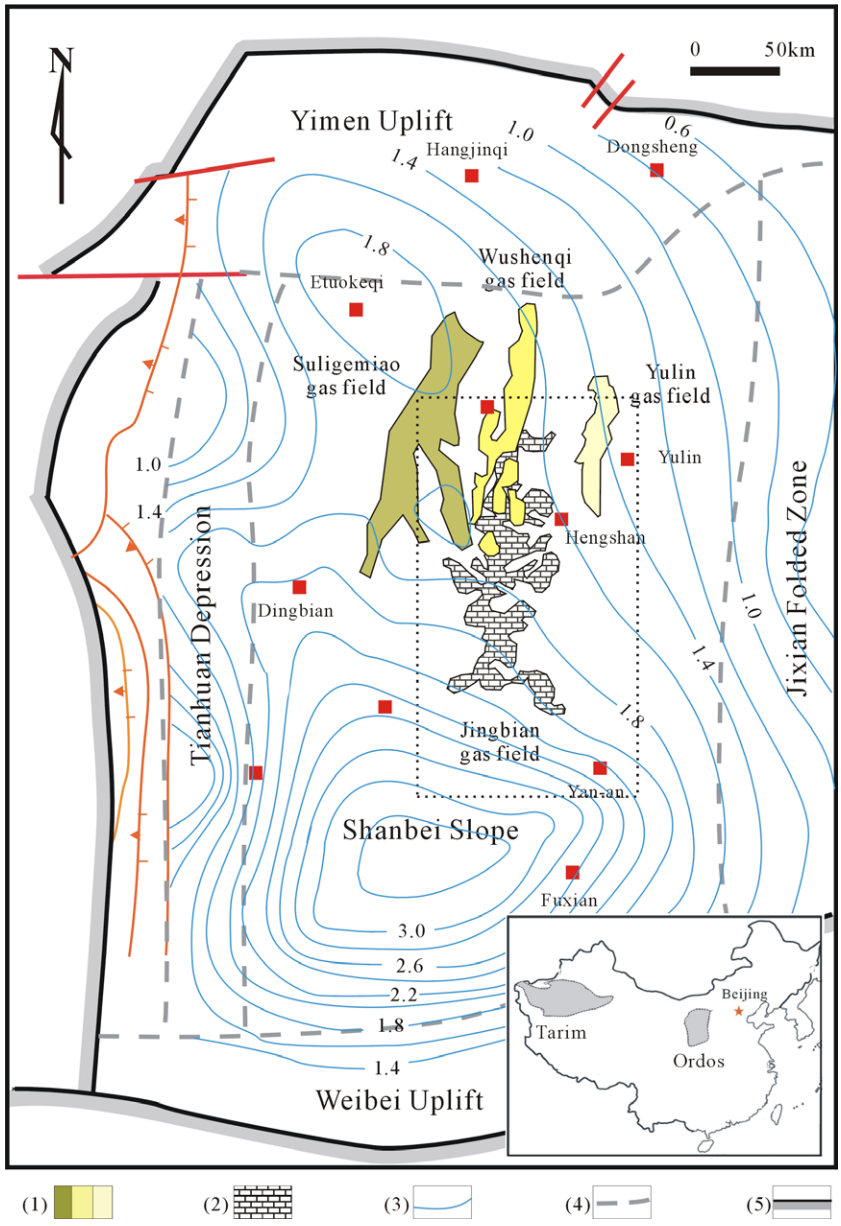

Fig. 7. Map showing the gas field locations in the Ordos Basin: (1) gas fields of Carboniferous–Permian reservoirs; (2) gas field of the Ordovician carbonate reservoirs; (3) vitrinite reflectance isoline (%Ro) on the base of the Permian strata at 97 Ma; (4) division of structural unit; (5) basin boundary.

Table 4
Simplified stratigraphic system of Ordos Basin

Strata		Formation	Code	Thickness (m)	Facies	Lithology	Note
Permian	Upper	Shiqianfeng Fm	P2s	200–345	Terrestrial river-lake facies	Lacustrine sandstone and mudstone	Seal
		Shangshihezi Fm	P2sh	130–160			
	Lower	Xiashihezi Fm	P1x	140–160			Gas reservoir
		Shanxi Fm	P1s	90–120	Marine shore plain and swamp	Alternating marine and terrestrial sandstone, mudstone, coal and limestone	Source rock
Carboniferous	Upper	Taiyuan Fm	C3t	60–80			
	Middle	Benxi Fm	C2b	10–40			
Ordovician	Lower	Majiagou Fm	O1m	108–896	Platform carbonate	Limestone, argillaceous dolomite	Gas reservoir

Table 5
Carbon isotope composition of the Permian reservoir gases from the Yulin, Wushenqi and Suligemiao gas fields

Field	Well	Code	Depth (m)	Carbon isotope composition (PDB, ‰)		
				$\delta^{13}C_1$	$\delta^{13}C_2$	$\delta^{13}C_3$
Yulin	S142	P_1s	2800.2–2813.5	−32.4	−26.1	−24.9
	S143	P_1s	2795.0–2812.6	−33.6	−26.0	−24.4
	S141	P_1s	2797.2–2828.6	−33.7	−26.3	−24.3
	S118	P_1s	2856.8–2364.0	−33.2	−25.8	−24.4
	S117	P_1s	2914.0–2928.0	−32.2	−26.0	−24.9
Wushenqi	S165	P1x	3103.2–3133.7	−33.0	−24.0	−24.5
	S167	P1x	3118.0–3126.4	−33.8	−23.5	−23.4
	S178	P1x	2990.8–2997.4	−34.2	−23.7	−23.7
	S231	P1x	3127.0–3146.6	−33.0	−24.4	−25.4
	S240	P1x	3157.8–3161.0	−31.4	−24.3	−24.6
	S241	P1x	3153.2–3196.8	−32.6	−24.1	−24.2
	S243	P1x	3042.2–3080.2	−35.0	−24.0	−23.6
Suligemiao	Su1	P1x	3350.0 – 3353.6	−34.2	−22.2	−22.1
	Su1	P1s	3656.8 – 3660.0	−34.4	−22.1	−21.8
	Su6	P1x	3319.5 – 3329.0	−33.5	−24.0	−24.7
	Su6	P1s	3377.0 – 3382.0	−33.9	−23.7	−24.2
	Su14	P1x	3503.0 – 3506.5	−32.5	−23.2	−23.8
	Su20	P1x	3442.1 – 3472.4	−33.0	−24.4	−24.7
	Tao5	P1x	3272.0 – 3275.0	−33.1	−23.6	−23.7

gases collected from the four giant gas fields, integrated after Dai et al. (2005), Cai et al. (2005) and Chen and Hu (2002). Several patterns of the carbon isotope-type curve are observed, suggesting gases are not generated from a single source rock or underwent post-genetic alteration (Figs. 8–11 and 13).

5.2. Natural gas in the sandstone reservoir – the isotope curve patterns for coal-derived gas and secondary cracking

The reservoir rocks of three giant gas fields, Yulin, Wushenqi and Suligemiao gas fields, are the C-P sandstone. It has been widely accepted that the natural gases of these gas fields were generated from the Carboniferous–Permian coal measures. However, different patterns of the 'natural gas plot' are still observed.

In the Yulin gas field, the carbon isotope compositions of methane, ethane and propane are −31.6‰ to −33.7‰, −25.8‰ to −26.3‰ and −23.8‰ to 24.9‰, respectively. They are within the isotope range of coaly gas. The isotope-type curve shows a typical coal-derived gas (Fig. 8), which supports strongly that the natural gas is derived from the C-P coal-bearing measure.

The other two gas fields, Wushenqi and Suligemiao, have also the C-P sandstones as reservoirs.

Table 6
Carbon isotope composition of the reservoir gases in the Jingbian gas field

Well	Code	Depth (m)	Carbon isotope composition (PDB, ‰)			Remark
			$\delta^{13}C_1$	$\delta^{13}C_2$	$\delta^{13}C_3$	
S19	C2b	3355.0 –3359.0	−35.4	−25.8	−24.9	C-P reservoir
S26	P1t	3407.4–3411.4	−33.5	−23.2	−23.0	
S16	Pls	2936.0–2940.0	−31.3	−25.3	−25.8	
S19	P1x	3171.0–3176.0	−35.1	−24.9	−24.5	
S41	P1s	3100.0–3104.0	−33.4	−24.6	−25.0	
S46	P1s	3214.0–3217.6	−31.0	−22.7	−21.3	
S65	P1x	3149.0–3154.0	−29.1	−23.5	−25.5	
S67	P1s	3618.5–3623.0	−32.5	−22.2	−21.9	
SC-1	O1m5	3443.0–3472.0	−33.9	−27.6	−26.0	Ordovician reservoir gas without the effective cap rock around Well SC-1
L1	O1m5	3431.9–3500.0	−33.7	−27.8	−25.6	
L2	O1m5	3190.0–3195.0	−35.2	−25.9	−25.4	
S2	O1m5	3364.4–3369.4	−35.3	−26.2	−25.5	
S12	O1m5	3638.0–3700.0	−34.2	−25.5	−26.4	
S21	O1m5	3292.0–3333.0	−34.5	−28.3	−27.1	
S27	O1m5	3360.0–3366.0	−36.8	−28.5	−26.4	
S28	O1m5	n.d.[a]	−36.2	−23.7	−23.5	
S33	O1m5	3560.2–3614.2	−35.0	−26.7	−25.5	
S34	O1m5	3410.0–3413.0	−35.3	−25.5	−24.4	
S35	O1m5	3524.0–3528.0	−33.7	−26.3	−21.7	
S61	O1m5	3459.0–3506.0	−34.0	−27.7	−28.4	
S68	O1m5	3675.0–3681.0	−34.0	−23.5	−21.604	
S5	O1m5	3451.0–3550.0	−33.8	−31.3	−27.1	Ordovician reservoir gas far from Well SC-1
S6	O1m5	n.d.	−33.9	−30.1	−24.4	
S13	O1m5	3394.0–3445.0	−31.6	−31.4	−28.8	
S14	O1m5	3703.0–3754.0	−32.9	−32.5	−25.1	
S15	O1m5	3521.0–3560.0	−33.2	−33.3	−25.9	
S17	O1m5	3176.9–3182.0	−33.3	−30.2	−27.8	
S20	O1m5	3561.0–3565.0	−34.2	−31.3	−26.4	
S22	O1m5	3327.0–3332.0	−33.9	−31.8	−27.2	
S23	O1m5	3412.6–3477.6	−33.1	−31.8	−27.1	
S24	O1m5	3315–3375	−32.5	−28.7	−26.4	
S25	O1m5	3486.0–3500.0	−33.3	−33.5	−28.1	
S30	O1m5	3643.0–3659.0	−33.1	−33.6	−26.5	
S31	O1m5	3521.0–3562.0	−32.1	−30.5	−26.3	
S44	O1m5	3414.0–3461.0	−33.0	−34.9	−29.9	
S45	O1m5	3245.0–3298.0	−33.5	−30.6	−22.9	
S49	O1m5	n.d.	−33.4	−31.8		
S51	O1m5	3690.0–3694.0	−34.0	−31.8	−25.0	
S62	O1m5	n.d.	−32.7	−33.1	−30.0	
S63	O1m5	3745.3–3750.5	−32.8	−30.5	−28.7	
S84	O1m5	n.d.	−31.8	−28.5	−24.2	
S93	O1m5	3503.2–3540.9	−31.7	−33.6	−27.6	
S102	O1m5	3370.4–3423.0	−32.6	−33.9	−24.3	
S106	O1m5	3224.6–3237.0	−30.7	−37.5	−29.9	
S154	O1m5	3154.0–3164.0	−32.6	−30.7	−27.2	
S155	O1m5	3217.3–3229.6	−33.1	−30.3	−27.3	
S26	O1	3534.3	−43.6	−23.3	−24.3	Fluid inclusions
S54	O1	4101.5	−33.3	−25.8	−26.3	
Sheng8	O1	2289.0	−41.1	−22.5	−21.4	

[a] No data.

The isotope-type curves are obviously different from that of Yulin Field. Although the methane carbon isotope compositions suggest that the gases of Wushenqi and Suligemiao fields are from the same source rock as Yulin gases, i.e. the C-P coal measure, the heavy hydrocarbon gases (ethane and

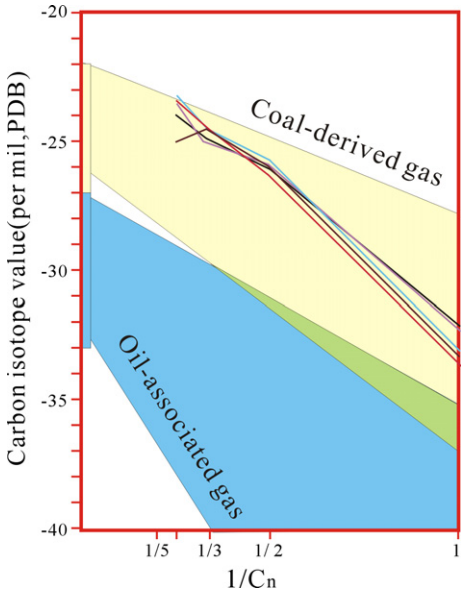

Fig. 8. 'Natural gas plot' of the Yulin gas field. The carbon isotope compositions of C_1–C_3 gaseous hydrocarbons are within the coal-derived gas range and a typical isotope-type curve of coal-derived gas is shown.

propane) are richer in ^{13}C than those of the Yulin gases and their values are above the isotope range of coal-derived gas (Fig. 9).

The reasons that the heavy hydrocarbon gases become richer in ^{13}C are possibly: (1) microbial oxidation, suggested by Burruss et al. (2003); (2) TSR, (e.g. Krouse et al., 1988; Machel, 2001); and (3) secondary cracking, Zou et al. (2006) for instance.

Biological activity occurs below 80 °C (Head et al., 2003). The present burial depth of the C-P reservoir strata in Suligemiao and Wushenqi gas fields is generally >2500 m, mostly between 2800 and 3400 m. Since the whole basin was uplifted during late Cretaceous (97 Ma), the reservoir temperature has not been below 90 °C (Fu et al., 2003; Dai et al., 2005). In other words, the temperature has been above the temperature for microbial activity (Head et al., 2003). Therefore, the heavy carbon isotope compositions of ethane and propane are unlikely to result from microbial activity. The reservoir rocks of these two fields are the Permian sandstone and silty sandstone (Dai et al., 2005; Xiao et al., 2005); the seal rocks are the Permian lacustrine mudstone (Dai et al., 2005; Xiao et al., 2005). Although part of the reservoir is within the temperature range for TSR (100–140 °C) to occur (Machel, 2001), it is unlikely for TSR to take place in a sandstone reservoir because of the absence of sulphate. Therefore, no evidence supports TSR in either of these two gas fields. The burial depths of the reservoirs in Wushenqi and Suligemiao gas fields are generally deeper than that of the Yulin field, but the maximum temperatures that the reservoirs were

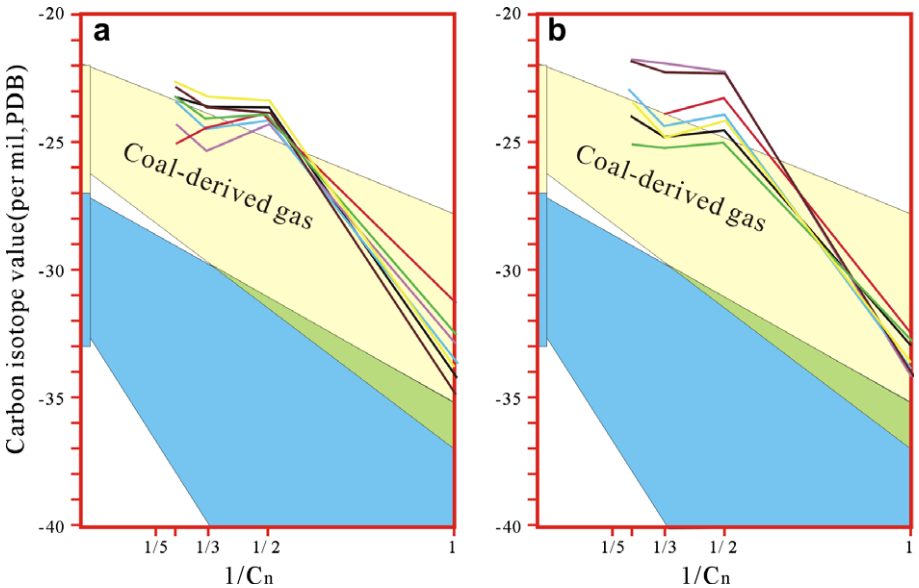

Fig. 9. Isotope-type curves of natural gas from Wushenqi (a) and Suligemiao gas field (b). The methane carbon isotope values are in the range of coal-derived gas; the carbon isotope values of both ethane and propane are above the range of coaly gas, suggesting secondary gas cracking.

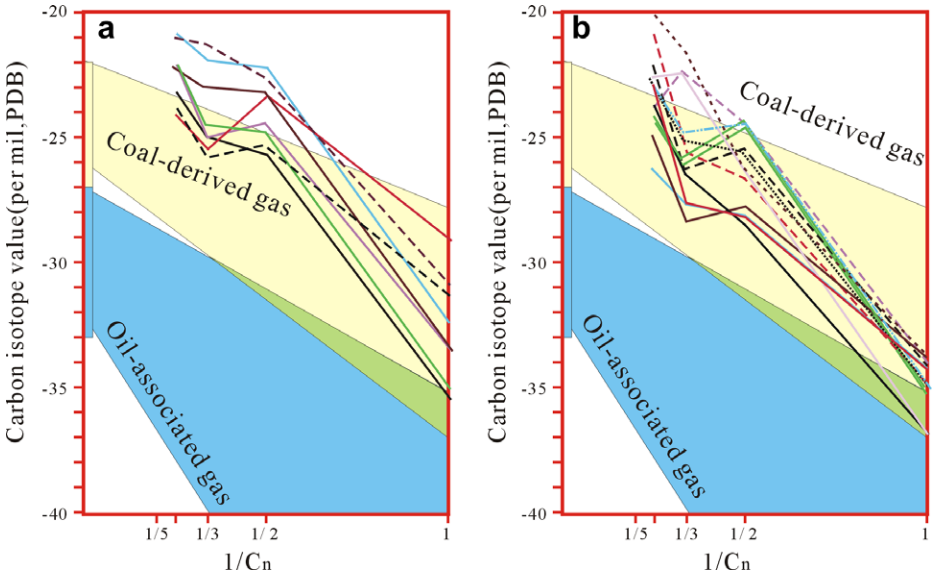

Fig. 10. Characteristic isotope curve of the gases around well SC-1 in the Jingbian gas field. (a) C-P sandstone reservoir gases. (b) Ordovician weathered crust gases.

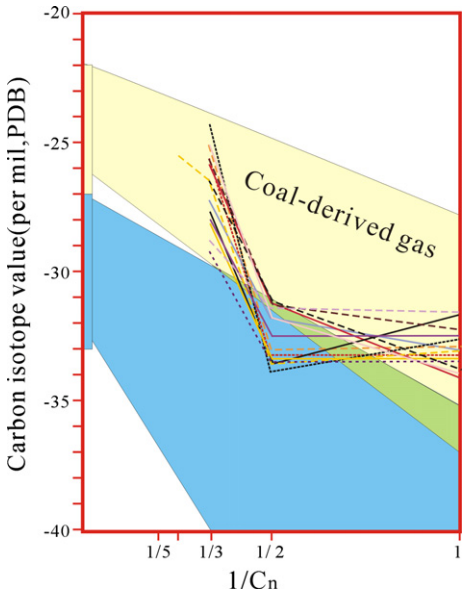

Fig. 11. Characteristic isotope curve of the gases in the Ordovician weathered crust reservoir far from Well SC-1. The relatively light isotope compositions of ethane and a concave isotope-type curve suggest that the gases are a mixture from oil- and gas-prone sources with high maturity.

exposed to were not more than 175 °C. Gas secondary cracking in the reservoirs is unlikely in the two gas fields. The source rock maturities of the Wushenqi and Suligemiao gas fields are relatively higher than that of the Yulin gas field. The vitrinite reflectance of the source rock for the Yulin gas field is 1.3–1.5%R_0, while the reflectance of the source rocks for the Wushenqi and Suligemiao gas fields is 1.6–2.0%R_0 (Fig. 7). Toward the south, the maturity increases to more than 2.0%R_0, covering a large area in the dry gas stage (Fig. 7). The most likely cause of the heavy ethane and propane isotope is secondary gas cracking within the source rock, which agrees with the experimental results (Fig. 4b).

5.3. Natural gas in the Ordovician carbonate reservoir – the pattern of isotope-type curve for mixing

The reservoir strata of the Jingbian gas field are mainly the Ordovician carbonates. From the end of the Ordovician to the middle Carboniferous, the whole basin was uplifted and exposed. Consequently, these strata underwent weathering and erosion, forming a 40–50 km wide weathered residue that was overlain by the C-P sequence (Cai et al., 2005). The weathered carbonate beneath the Carboniferous/Ordovician unconformity, the so-called weathered crust, became the main reservoir strata of this field. The cap rock is a bauxitic mudstone beneath the unconformity/coal measure for the top gas pools as well as argillaceous dolomite and marlstone for other gas pools. The C-P sandstone reservoir is distributed in a limited area of this field.

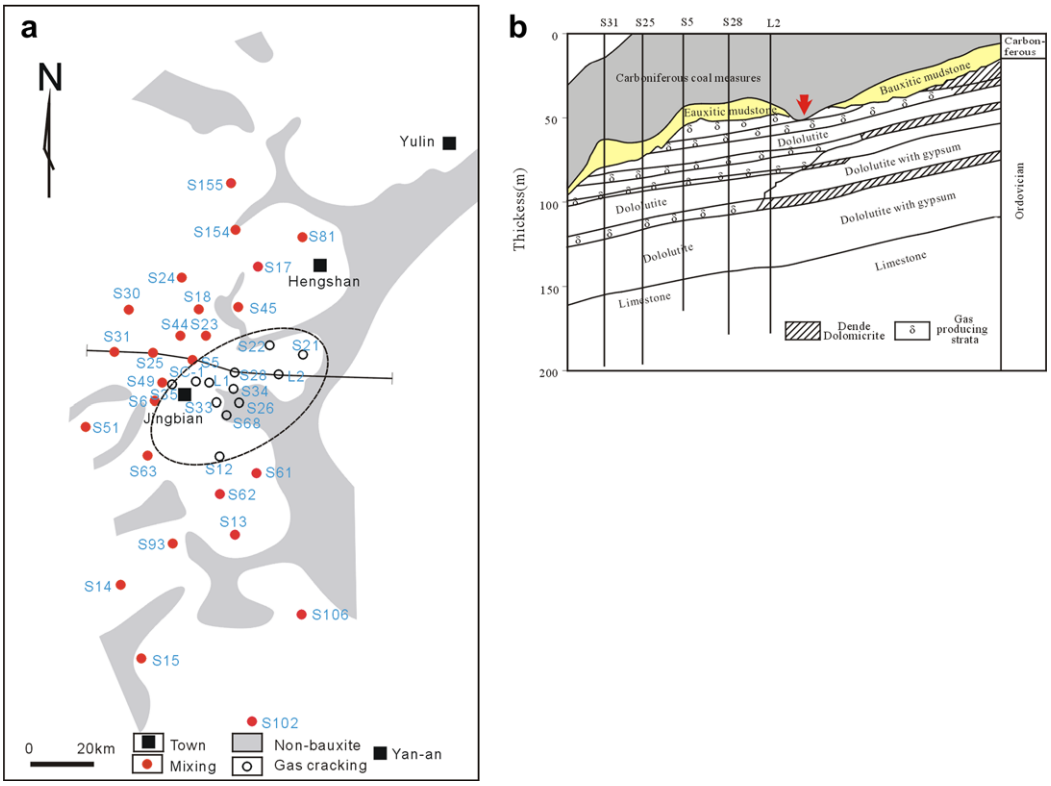

Fig. 12. (a) Map showing the bauxite seal distribution of the Ordovician reservoir (modified after Li et al., 2002) and isotope-type curves. The C-P coal-derived gas (open circle) stored in the Ordovician weathered crust reservoir occurs around Well SC-1, while mixed gas (solid circles) occurs far from this well, suggesting that there is a channel for coaly gas to enter the Ordovician reservoir. The location of the Jingbian Gas Field in the Ordos Basin is shown in Fig. 7 (dashed box). (b) A cross-section showing the position of the reservoirs, the bauxite seal, the source rocks, indicating the potential channel (arrow) for coaly gas migration downwards into the Ordovician reservoir.

The origin of the gas produced from the Ordovician reservoirs remains enigmatic (Cai et al., 2005). There is no consensus on the source of the gases in the Jingbian gas field (Dai et al., 2005). The isotope-type curves of the natural gases from the Jingbian Field are complex, as demonstrated by Dai et al. (2005). In this paper, the carbon isotope data from the Jingbian Field, after Dai et al. (2005) and Cai et al. (2005), are divided into three groups according to reservoir age and sites (Table 6). The carbon isotope values of the hydrocarbon gases from fluid inclusions (Chen and Hu, 2002) are also presented in Table 6.

The patterns of the isotope plots of natural gases from the Ordovician carbonate reservoir are displayed in Fig. 10, and could provide a key to their origins. Fig. 10 illustrates the isotope-type curve of the gases around Well SC-1 in the Jingbian gas field (Fig. 10), which shows the isotope-type curve pattern of the C-P sandstone reservoir gases in the Jingbian Field (Fig. 10a) which are very similar to those of the C-P sandstone reservoirs in the Wushenqi and Suligemiao Fields (Fig. 9), suggesting both their identical origin and post-genetic alteration. In other words, all the natural gas discovered in the C-P sandstone reservoir of this basin was generated from the C-P coal measure. Interestingly, the Ordovician weathered crust gases (Fig. 10b) around this site also demonstrate the same patterns of isotope-type curve as the C-P sandstone reservoir gases (Fig. 10a), revealing a genetic relationship between the gases in the Ordovician carbonate and in the C-P sandstone reservoirs. Thus, the Ordovician weathered crust gases around Well SC-1 in the Jingbian Field appear to originate also from the C-P coal measure.

In contrast, a drastically different pattern of the isotope curve is exhibited by the Ordovician weathered crust gases far from Well SC-1 (Fig. 11), indicating the gas sources and post-genetic alterations

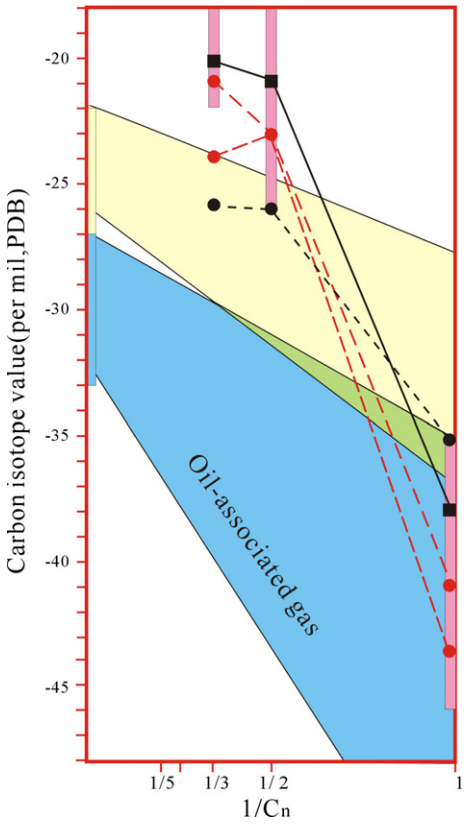

Fig. 13. Characteristic isotope curves of fluid inclusions and thermochemical sulphate reduction (TSR). Filled boxes: the carbon isotope range of TSR (data after Machel, 2001); solid squares: a case of the characteristic isotope curve resulting from TSR (redrawn after Krouse et al., 1988); solid circles: carbon isotope compositions of fluid inclusions (data after Chen and Hu, 2002). One fluid inclusion falls into the coal-derived gas area and the two others are within the TSR area. Both TSR and coal-derived gas during geological history are recorded in fluid inclusion isotope compositions.

are different from the C-P reservoir gases. The Ordovician weathered crust gases far from Well SC-1 have heavy propane and methane isotopes; concave isotope-type curves are observed (Fig. 11). However, the ethane isotope is still within the range of oil-associated gas, indicating ethane is from oil-prone source rock. As stated above, the concave isotope-type curve may be caused by (1) gas leakage/diffusion; (2) high maturity oil-associated gas or (3) admixture of high maturity oil- and coal-associated gases.

According to the research performed by Clayton et al. (1997), Prinzhofer and Pernaton (1997) and Zhang and Krooss (2001), diffusive leakage may result in a ^{13}C enrichment of the residual methane whereas the isotopic composition of propane should hardly change. In this case, isotopic composition of propane goes beyond the boundary of oil-associated gas, but ethane isotope is still within the range of oil-associated gas, which suggests that the Ordovician weathered crust gases far from Well SC-1 are affected by a diffusive leakage process. Although high maturity oil-associated gases may have heavy propane isotope isotopic compositions, exceeding the boundary of the characteristic field, the corresponding isotopic composition of methane remains usually within the range of oil-associated gas. Obviously, the weathered crust gases do not originate from one high maturity oil-prone source. Fig. 11 shows that all methane isotopes are within the range of coal-derived gas, suggesting methane origin is associated with coal measures. The most likely scenario is that the weathered crust gases far from Well SC-1 are mixtures of overmature oil- and coal-associated gases.

The bauxite seal distribution on the top of the Ordovician weathered crust reservoir is demonstrated in Fig. 12a. When the Carboniferous sequence was deposited, part of the bauxite on the Ordovician weathered crust was eroded, then filled with the Carboniferous mudstone or sandstone (Li et al., 2002), which partly replaced the bauxite as the cap rock of the Ordovician gas pool. The sealing capability of the Carboniferous sandstone/mudstone is less than that of the Ordovician bauxite, resulting in the migration of coal-derived gas of high maturity into the Ordovician reservoir of the Jingbian Field (Fig. 12b). Consequently, the carbon isotope compositions of methane in the Wushenqi, Suligemiao and Jingbian gas fields are very similar to each other (mainly $-32‰$ to $-34‰$), whereas the gas fractionation during expulsion and secondary migration (Snowdon, 2001) leads to predominantly methane migration into the Ordovician reservoir. Thus, the carbon isotope compositions of ethane and propane were less affected by the C-P gas. Therefore, the ethane and propane of the Ordovician reservoir gases keep the isotope characteristics of oil-associated gas with high maturity and the methane shows the influence of the isotope characteristics of coal-derived gas, resulting in the difference pattern of isotope-type curves from the C-P reservoir gases. The geological analysis further supports that the Ordovician weathered crust gases far from Well SC-1 are mixed gases from high maturity oil- and gas-prone sources. This is due to the erosion and the low seal quality of the Carboniferous strata that form a 'window' around Well SC-1, which

becomes a channel for the C-P gases to enter the Ordovician reservoirs. Thus, a special scenario, in which both the C-P gases and the Ordovician gases have the same isotopic pattern, is observed. As illustrated in Fig. 12a, the coal-derived gas is limited around Well SC-1 between Hengshan and Jingbian Counties, whereas the mixed gas is distributed in a wide area far from Well SC-1.

5.4. Did TSR occur in the Ordovician carbonate reservoir?

Important information on the chemical components and isotope compositions of natural gas can be obtained from fluid inclusions in the reservoir (Thiery et al., 2000). Chen and Hu (2002) collected several samples from a calcite vein that occurred in the fractures of the Ordovician Jingbian Field reservoir. The gases in fluid inclusions were released by means of vacuum ball grinding, and then the carbon isotope compositions of the hydrocarbon gases were measured. The gases in the fluid inclusions were classified as coal-derived gas because of their heavy ethane isotope compositions (Chen and Hu, 2002). Based on the C_1–C_3 carbon isotope values of the gaseous hydrocarbons of these fluid inclusions, Cai et al. (2005) concluded that TSR took place in the Ordovician carbonate reservoir and resulted in the hydrocarbon gas becoming methane enriched with isotopically heavier carbon and an increasing dryness coefficient.

The isotope-type curves of the fluid inclusions are shown in Fig. 13, in which the carbon isotope range of TSR described by Machel et al. (1995) and Machel (2001) and a TSR case provided by Krouse et al. (1988) are also illustrated for comparison. Both patterns of isotope-type curves, coal-derived gas and TSR, are shown in Fig. 13.

The carbon isotope compositions of the C_1–C_3 gases in the fluid inclusions suggest that TSR took place in the Ordovician carbonate reservoir. However, the same isotope-type curve pattern is not observed in numerous wells and pool gases. In contrast, a concave isotope-type curve with light ethane isotope value is prevalent in the Ordovician carbonate reservoir (Fig. 11), which seems to indicate that the TSR is uncommon in this reservoir.

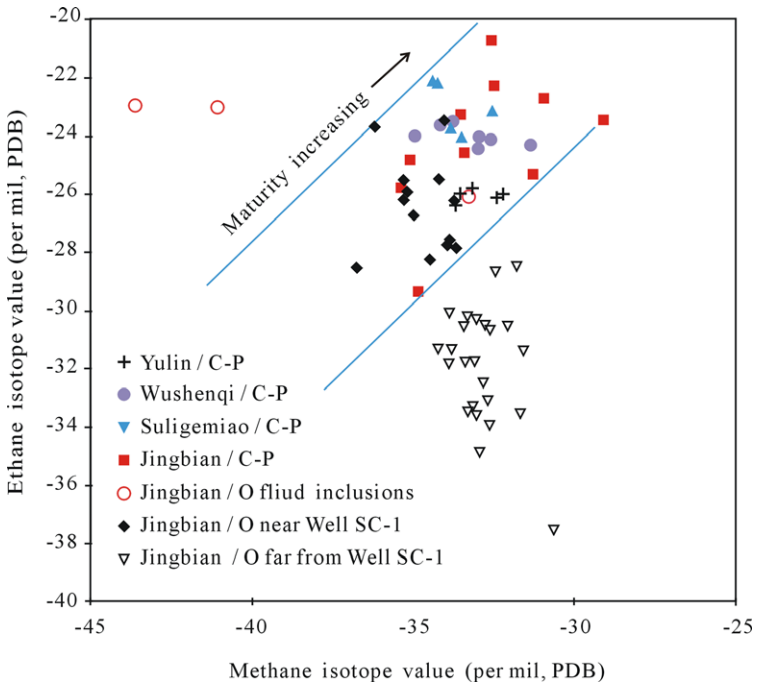

Fig. 14. Methane isotope vs. ethane isotope diagram. The gases in the C-P reservoirs, the Ordovician reservoir near Well SC-1 and one fluid inclusion are coal-derived gases. The gases of the other two fluid inclusions have obviously distinctly different characteristics (TSR). The other gases in the Ordovician reservoirs of the Jingbian gas field show a trend of gradually approaching the C-P reservoir gases, indicating an increase in coaly gas in the gas mixture.

An alternative explanation for the increasing dryness coefficient is the mixing of coal-derived methane as well as C_{2+} cracking in the reservoir. The methane vs. ethane isotope diagram of natural gases from different gas fields/reservoirs of the Ordos Basin is illustrated in Fig. 14, which shows three clusters among them, the gases in the C-P reservoirs, the Ordovician reservoir near Well SC-1, and one fluid inclusion have a characteristic increase of methane isotopes as ethane isotope value increase, demonstrating a maturity trend and a genetic relationship between them. The other two gases from fluid inclusions and the other gases in the Ordovician reservoirs of the Jingbian Field are far from this cluster, suggesting their different origins and/or post-genetic alterations.

6. Conclusions

On the basis of statistical and pyrolysis experimental data, the carbon isotope range and boundary of hydrocarbon gases generated from gas-prone and oil-prone source rocks are used to modify the 'natural gas plot' proposed originally by Chung et al. (1988). Deviation from the typical patterns may be caused by heavy hydrocarbon gas cracking, thermochemical sulphate reduction, and mixing as discussed using a case study in this paper. The following origins and post-genetic alterations of natural gas are recognized by applying these patterns to the Ordos Basin:

(1) Different isotope patterns result from secondary cracking and TSR. A convex curve with heavy ethane and propane isotope values is indicative of coal-derived gas cracking and TSR because of catalysis in reservoirs. In contrast, a concave curve with large differences between ethane and propane isotopes is found when oil-associated gas secondary cracking occurred.
(2) The natural gas discovered in the Yulin gas field is a typical coal-derived gas, generated from the Carboniferous–Permian coal-bearing measures. The natural gases in the Wushenqi and Suligemiao gas fields are highly mature coal gases. The heavy carbon isotope compositions of ethane and propane are thought to be caused by secondary cracking of C_{2+} hydrocarbons.
(3) Mixing of oil-associated gas and coal-derived gas takes place in the Ordovician reservoirs of the Jingbian gas field, while the natural gas around Well SC-1, whether found in the Ordovician or in the C-P reservoirs, is mainly from the C-P coal measures. In the gas mixture, methane is mainly from the C-P coal measures and the C_{2+} gaseous hydrocarbons are generated from highly mature carbonate.
(4) The isotope-type curves of the hydrocarbon gases from fluid inclusions suggest that TSR took place in the Ordovician carbonate reservoir of the Jingbian Field during its geologic history, but those of the reservoir gases show that TSR is less common in gas pools. The increasing dryness may be related to methane mixed from the C-P coal-derived gas and heavy gaseous hydrocarbon cracking in the Ordovician reservoir.

Acknowledgements

We thank Drs. J.Z. Liu and W.L. Jia for their assistance in carrying out pyrolysis experiments and isotopic analysis. This work was supported financially by the Natural Sciences Foundation of China (Grant Nos. 40572083 and 40272067). Prof. Philip A. Meyers (University of Michigan, USA) is gratefully acknowledged for his comments and language improvements. The manuscript benefited greatly from the very careful and detailed reviews of two anonymous reviewers.

Associate Editor—**Maowen Li**

References

Andresen, B., Throndsen, T., Raheim, A., Bolstad, J., 1995. A comparison of pyrolysis products with models for natural gas generation. Chemical Geology 126, 261–280.

Behar, F., Vandenbroucke, M., Tang, Y., Marquis, F., Espitalie, J., 1997. Thermal cracking of kerogen in open and closed systems: determination of kinetic parameters and stoichiometric coefficients for oil and gas generation. Organic Geochemistry 26, 321–339.

Berner, U., Faber, E., Scheeder, G., Panten, D., 1995. Primary cracking of algal and landplant kerogens: kinetic models of isotope variations in methane, ethane and propane. Chemical Geology 126, 233–245.

Burruss, R.C., Lillis, P.G., Collett, T.S., 2003. Geochemistry of natural gas, North Slope, Alaska: Implications for gas resources, NPRA. U.S. Geological Survey Open-File Report 03-041. <http://pubs.usgs.gov/of/2003/of03-041>.

Cai, C., Hu, G., He, H., Li, J., Li, J., Wu, Y., 2005. Geochemical characteristics and origin of natural gas and thermochemical sulphate reduction in Ordovician carbonates in the Ordos Basin, China. Journal of Petroleum Science and Engineering 48, 209–226.

Chen, M., Hu, G., 2002. A new method in assaying gas isotopes in fluid inclusion and the way of application. Oil & Gas Geology 23, 339–342.

Chung, H.M., Gormly, J.R., Squires, R.M., 1988. Origin of gaseous hydrocarbons in subsurface environments: theoretical considerations of carbon isotope distribution. Chemical Geology 71, 97–103.

Clayton, C., 1991. Carbon isotope fractionation during natural gas generation from kerogen. Marine and Petroleum Geology 8 (2), 232–240.

Clayton, C.J., Hay, S.J., Baylis, S.A., Dipper, B., 1997. Alteration of natural gas during leakage from a North Sea salt diapir field. Marine Geology 137, 69–80.

Cramer, B., Faber, E., Gerling, P., Krooss, B.M., 2001. Reaction kinetics of stable carbon isotopes in natural gas-insights from dry, open system pyrolysis experiments. Energy & Fuels 15, 517–532.

Dai, J., 1999. Significant advancement in research on coal-formed gas in China. Petroleum Exploration and Development 26, 1–10.

Dai, J., Li, J., Luo, X., Zhang, W., Hu, G., Ma, C., Guo, J., Ge, S., 2005. Stable carbon isotope compositions and source rock geochemistry of the giant gas accumulations in the Ordos Basin, China. Organic Geochemistry 36, 1617–1635.

Duan, Y.C., 1995. Study of characteristics of coal isotope composition in China. Coal Geology and Exploration 23, 29–33 (in Chinese, English abstract).

Faber, E., Stahl, W., 1984. Geochemical surface exploration for hydrocarbons in the North Sea. American Association Petroleum Geologists Bulletin 68, 363–386.

Fu, S., Peng, P., Zhang, W., Liu, J., Li, J., Zan, C., 2003. Kinetic study of the hydrocarbon generation from Upper Paleozoic coals in Ordos Basin. Science in China (Series D) 46, 333–341.

Gaschnitz, R., Krooss, B.M., Gerling, P., Faber, E., Littke, R., 2001. On-line pyrolysis-GC-IRMS: isotope fractionation of thermally generated gases from coals. Fuel 80 (15), 2139–2153.

Head, I.M., Jones, D.M., Larter, S.R., 2003. Biological activity in the deep subsurface and the origin of heavy oil. Nature 426, 344–352.

Hosgomez, H., Yalcin, M.N., Cramer, B., Gerling, P., Mann, U., 2005. Molecular and isotopic composition of gas occurrences in the Thrace basin (Turkey): origin of the gases and characteristics of possible source rocks. Chemical Geology 214, 179–191.

Huang, D., Liu, B., Wang, T., Xu, Y., Chen, S., Zhao, M., 1999. Genetic type and maturity of Lower Paleozoic marine hydrocarbon gases in the eastern Tarim Basin. Chemical Geology 162, 65–67.

James, A.T., 1983. Correlation of natural gas by use of carbon isotope distribution between hydrocarbon components. American Association of Petroleum Geologists Bulletin 67, 1176–1191.

Jia, C.Z., Qin, S.F., Li, Q.M., 2000. Formation and distribution of coal-formed petroleum in the Kuqa foreland depression of Tarim Basin. In: Dai, J.X., Fu, C.D., Xia, X.Y. (Eds.), International Symposium on Hydrocarbon from Coal. Petroleum Industry Press, Beijing (in Chinese).

Katz, B.J., Narimanov, A., Huseinzadeh, R., 2002. Significance of microbial processes in gases of the South Caspian basin. Marine and Petroleum Geology 19, 783–796.

Krouse, H.R., Viau, C.A., Eliuk, L.S., Ueda, A., Halas, A., 1988. Chemical and isotopic evidence of thermochemical sulphate reduction by light hydrocarbon gases in deep carbonate reservoirs. Nature 333, 415–419.

Li, X-Q., Hu, G-Y., Zhang, A-Y., Li, J., 2002. The source of Lower Paleozoic natural gases in central gas field in Erdos. Geoscience 16, 191–198 (in Chinese, English abstract).

Liu, Q., Liu, W., Qin, S., Wang, W., Gao, B., 2002. Gas generating characteristics of coal rock and its maceral in thermal simulation. Petroleum Geology and Experiment 24, 147–151 (in Chinese, English abstract).

Liu, W.H., Song, Y., Liu, Q.Y., Qin, S.F., Wang, X.F., 2003. Evolution of carbon isotopic composition in pyrolytic gases generated from coal and its main macerals. Acta Sedimentologica Sinica 21, 183–190 (in Chinese, English abstract).

Lorant, F., Prinzhofer, A., Behar, F., Huc, A.Y., 1998. Carbon isotopic and molecular constraints on the formation and the expulsion of thermogenic hydrocarbon gases. Chemical Geology 147, 240–264.

Machel, H.G., 2001. Bacterial and thermochemical sulfate reduction in diagenetic settings – old and new insights. Sedimentary Geology 140, 143–175.

Machel, H.G., Krouse, H.R., Sassen, R., 1995. Products and distinguishing criteria of bacterial and thermochemical sulfate reduction. Applied Geochemistry 10, 373–389.

Mattavelli, L., Ricchiuto, T., Grignani, D., Cahoell, M., 1983. Geochemistry and habitat of natural gases in Po basin, Northern Italy. American Association Petroleum Geologists Bulletin 67, 2239–2254.

Pallasser, R.J., 2000. Recognising biodegradation in gas/oil accumulations through the $\delta^{13}C$ compositions of gas components. Organic Geochemistry 31, 1363–1373.

Pohlman, J.W., Canuel, E.A., Chapman, N.R., Spence, G.D., Whiticar, M.J., Coffin, R.B., 2005. The origin of thermogenic gas hydrates on the northern Cascadia Margin as inferred from isotopic ($^{13}C/^{12}C$ and D/H) and molecular composition of hydrate and vent gas. Organic Geochemistry 36, 703–716.

Prinzhofer, A., Vegab, M.A.G., Battanic, A., Escudero, M., 2000. Gas geochemistry of the Macuspana Basin (Mexico): thermogenic accumulations in sediments impregnated by bacterial gas. Marine and Petroleum Geology 17, 1029–1040.

Prinzhofer, A., Huc, A.Y., 1995. Genetic and post-genetic molecular and isotopic fractionations in natural gases. Chemical Geology 126, 281–290.

Prinzhofer, A., Pernaton, E., 1997. Isotopically light methane in natural gases: bacterial imprint or fractionation? Chemical Geology 142, 193–200.

Sassen, R., Milkov, A.V., Ozgul, E., Roberts, H.H., Hunt, J.L., Beeunas, M.A., Chanton, J.P., DeFreitas, D.A., Sweet, S.T., 2003. Gas venting and subsurface charge in the Green Canyon area, Gulf of Mexico continental slope: evidence of a deep bacterial methane source? Organic Geochemistry 34, 1455–1464.

Schoell, M., 1980. The hydrogen and carbon isotopic composition of methane from natural gases of various origins. Geochimica et Cosmochimica Acta 44, 649–661.

Schoell, M., 1983. Genetic characterization of natural gases. American Association Petroleum Geologists Bulletin 67, 2225–2238.

Snowdon, L.R., 2001. Natural gas composition in a geological environment and the implications for the processes of generation and preservation. Organic Geochemistry 32, 913–931.

Stahl, W., 1977. Carbon and nitrogen isotopes in hydrocarbon research and exploration. Chemical Geology 20, 121–149.

Stahl, W., Carey, B.D., 1975. Source-rock identification by isotope analyses of natural gases from fields in the Val Verde and Delaware basins, West Texas. Chemical Geology 16, 257–267.

Tang, Y., Perry, J.K., Jenden, P.D., Schoell, M., 2000. Mathematical modelling of stable carbon isotope ratios in natural gases. Geochimica et Cosmochimica Acta 64, 2673–2687.

Thiery, R., Pironon, J., Walgenwitz, F., Montel, F., 2000. PIT (Petroleum Inclusion Thermodynamic): a new modeling tool for the characterization of hydrocarbon fluid inclusions from volumetric and microthermometric measurements. Journal of Geochemical Exploration 69–70, 701–704.

Wang, J., Chen, J.F., 2004. Geochemical meaning and characteristics of carbon isotope composition of organic matter of pre-Cambrian in North China. Journal of Mineral Petrology 24, 83–87 (in Chinese, English abstract).

Whiticar, M.J., 1999. Carbon and hydrogen isotope systematics of bacterial formation and oxidation of methane. Chemical Geology 161, 291–314.

Xiao, X.M., Zhao, B.Q., Thu, Z.L., Song, Z.G., Wilkins, R.W.T., 2005. Upper Paleozoic petroleum system, Ordos Basin, China. Marine and Petroleum Geology 22, 945–963.

Zhang, T., Krooss, B.M., 2001. Experimental investigation on the carbon isotope fractionation of methane during gas migration by diffusion through sedimentary rocks at elevated temperature and pressure. Geochimica et Cosmochimica Acta 65, 2723–2742.

Zou, Y.-R., Wang, L.Y., Shuai, Y.H., Peng, P.A., 2005. EasyDelta: a spreadsheet for kinetic modeling of the stable carbon isotope composition of natural gases. Computers & Geosciences 31, 811–819.

Zou, Y.-R., Zhao, C., Wang, Y., Zhao, W., Peng, P., Shuai, Y., 2006. The characteristics and origin of natural gases in Kuqa depression, Tarim Basin, NW China. Organic Geochemistry 37, 280–290.